

Prediction of Macroscopic Properties of Protic Ionic Liquids by Ab Initio Calculations

Henrik Markusson,^{*,†} Jean-Philippe Belières,[‡] Patrik Johansson,[†] C. Austen Angell,[‡] and Per Jacobsson[†]

Department of Applied Physics, Chalmers University of Technology, SE-412 96 Göteborg, Sweden, and Department of Chemistry and Biochemistry, Arizona State University, Tempe Arizona 85287-1604

Received: March 13, 2007; In Final Form: July 2, 2007

We have systematically investigated combinations of anions and cations in a number of protic ionic liquids based on alkylamines and used ab initio methods to gain insight into the parameters determining their liquid range and their conductivity. A simple, almost linear, relation of the experimentally determined melting temperature with the calculated volume of the anion forming the ionic liquid is found, whereas the dependence of the melting temperature with increasing cation volume goes through a minimum for relatively short side chain length. On the basis of the present results, we propose a strategy to predict the nature of protic ionic liquids in terms of low vapor pressure and conductivity. Comparisons with previously reported strategies for prediction of melting temperatures for aprotic ionic liquids are also made.

I. Introduction

The usefulness of ionic liquids (ILs), materials composed entirely of ions that are fluid at temperatures below 100 °C,¹ has in recent years been recognized in many fields of science and technology. As a result, the number of compounds classified as ILs has grown exponentially. ILs, with their readily adjustable properties, are now used with success as “green” solvents in chemical process industries where they replace the conventional volatile solvents at the same time as they simplify separation of the products and increase the yield.^{1,2} Another area where they have received a lot of recent attention concerns electrochemical devices. The main reasons why ILs are promising in such applications are their inflammability, high ionic conductivity, and very low vapor pressures.³ This means that energy conversion devices based on these materials as electrolytes can be made considerably safer and can have improved performance compared with the conventional aqueous and nonaqueous electrolytes used today.

Most of the ILs studied for use in electrochemical devices are aprotic and studied for battery application purposes,^{4,5} but recently protic ILs (PILs) were proposed⁶ and tested as fuel cell (FC) electrolytes.⁷ This is due to their proton conducting properties, the very low vapor pressure even at temperatures above the boiling point of water, and their wide liquid temperature range (up to 350 °C⁸). Replacing the water-based low-temperature FC systems of today with PIL based electrolytes could thus increase their working temperatures to well above 100 °C, reducing the catalyst poisoning problem and subsequently reduced load demands. In addition, the replacement circumvents many of the unsolved problems of water management in the polymer electrolyte membrane FC's of today. The working temperature range of a PIL is set by the melting temperature (T_m) and its boiling point or its decomposition temperature. These temperatures can vary substantially between

different PILs, for reasons presently not fully understood and is therefore a subject of study in this work.

PILs are formed by transfer of a proton from an acid (AH) to a base (B) of a Brønsted acid–base pair. In the aprotic ILs the transferred species is any group of higher complexity than a proton. PILs often have higher conductivities and fluidities than the aprotic ILs. The PILs, where the sizes of the ions are small, also tend to melt at lower temperatures than their aprotic analogues.⁹ The obvious difference of the PILs compared with aprotic ILs is the reversible hydrogen transfer between the acid and the base. This implies that for PILs where the transfer is weak the properties are closer to the corresponding binary liquid, e.g., a non-negligible vapor pressure at elevated temperatures,¹⁰ whereas the aprotic ILs keep their ionic character until decomposition. Previously some of us reported that for PILs the degree of proton transfer, measured as the aqueous acidity difference (ΔpK_a), influences the excess boiling point (the increased boiling temperature, compared to the arithmetic mean of the boiling temperature of the acid and base).¹⁰ As the proton-transfer free energy increases, the PILs become more similar to aprotic ILs in terms of ionic character.

A crucial demand on a PIL for FC application is high proton conductivity. This demands the high fluidity or high diffusion rate of the proton transporting species. High proton conductivity can also come from proton hopping, or Grotthuss,¹¹ mechanisms. For hopping to occur in PILs based on amines, with only one acceptor site for the proton, the proton has to be able to hop back and forth between the acid and the base. This will not happen in systems with complete proton transfer, nor will it happen in acid base binary mixtures. The maximum hopping will occur for intermediate proton-transfer ratios, where the energy needed to transfer the proton should only equal the activation energy. The energy for the proton transfer is also important at the electrodes where the protons are transferred to and from the electrolyte. It is thus likely that the degree of proton transfer is important for the oxygen overpotential in PIL based FC.⁸

The properties of different ILs can vary substantially. It is therefore of utmost importance to find a simple and cost-

* Corresponding author. Fax: +46 (0)31 772 20 90. Phone: +46(0) 31 772 31 78. E-mail: henrik.markusson@fy.chalmers.se.

[†] Chalmers University of Technology.

[‡] Arizona State University.

TABLE 1: T_m , ΔT_m , and ΔE for PILs of Different Acids and Bases

acid	pK_a^{23-25}	T_m (°C)				ΔT_m (°C)				ΔE (kJ mol ⁻¹) B = EA
		NH ₃	MA	EA	BA	NH ₃	MA	EA	BA	
formic acid, HCOOH	3.75	120	-22	-73	-47	155	21	-37	-26	507
hydrofluoric acid, HF ^a	3	125	-11	4		206	76	85		411
phosphoric acid, H ₃ PO ₄	2.12	193	97	110	114	211	122	129	118	427
sulfamic acid, H ₂ NSO ₃ H	1	133		61	88	70		-2	10	395
tetrafluoroboric acid, HBF ₄	0.5	230	188	152	198	314	280	240	268	^b
trifluoroacetic acid, CF ₃ COOH	0.5, 0.23, -0.25	125		54		172		102		416
nitric acid, HNO ₃	-1.3	169	105	13	>20 ^c	254	197	99		420
methanesulfonic acid, CH ₃ SO ₃ H	-0.6, -2.6	183	91	113	132	212	128	143	147	406
sulfuric acid, H ₂ SO ₄	-3, -9	116	73	32	34	150	115	67	53	366
triflic acid, CF ₃ SO ₃ H	-14, -16	225		172		242	-	190		320

^a Stoichiometric ratio of 2:1 is needed for HF neutralization reaction with an amine. ^b HBF₄ decomposes into HF and BF₃ upon optimization on all calculational levels used, thus ΔE could not be calculated. ^c A melting temperature of above room temperature is given in ref 49.

effective way to screen the optimal properties of new ILs without going through the slow process of synthesizing each combination. There are many recent studies in the literature where calculations have been applied to the ionic liquid field to gain insight into, for instance, conductivity or melting temperature.¹²⁻¹⁵ A very recent study by Krossing et al. uses lattice and solvation free energies to explain the melting temperature in ILs.¹⁶ However, none of the calculational studies mentioned above concerns PILs, and our goal here is to calculate molecular level properties of PILs and draw conclusions on their melting temperature and conductivity determined from experiments.

Lately the interest in PILs has increased but so far the most extensive experimental work has been conducted in one of our labs.^{6,8,9} A few additional studies mostly concerning imidazolium based IL are available¹⁷⁻²⁰ including one study by Susan et al. of different PILs composed of the acid bis(trifluoromethanesulfonyl)imide (HTFSI) and various amines.⁷ Here they reported successful FC tests using the Im/HTFSI PIL as electrolyte, although with a high overpotential. It has been reported that imidazolium poisons the electrode,²¹ arguably by binding strongly to the platinum (111) surface²² and subsequently imidazolium ILs are excluded in our study. Our experimental work includes a large number of combinations of acids and bases and makes an excellent data base for systematic comparisons with calculational results. Although some of the compounds in this study have $T_m > 100$ °C we choose to call all of them PILs, for brevity.

In our present calculations we consider acid/base (1:1) pairs, and the separate acids and bases, in the gas phase, with focus on monosubstituted alkylamine bases. With this simple model it is possible to investigate many different acid base pairs as the degrees of freedom for the system are at an acceptable level. We investigate what factors that determine the FC working temperature of PILs, and also how the extent of proton transfer affects the conductivity, and finally give recommendations on how to design PILs with high conductivities within a desired temperature range.

II. Calculational and Experimental Details

II.a. Materials. The main system of study are PILs of the common base ethylamine (EA) and acids (AH) of varying aqueous acidity (pK_a) following the series formic acid < hydrofluoric acid < phosphoric acid < sulfamic acid < tetrafluoroboric acid < trifluoroacetic acid < methanesulfonic acid < nitric acid < sulfuric acid < triflic acid (Table 1).²³⁻²⁵ However, the pK_a value of the hydrofluoric acid (HF) is misleading, as HF is the strongest acid of them all if measured by the Hammett acidity function ($H_0 = -15.1$ for HF vs -14

for triflic acid).²⁶⁻²⁸ For a majority of the acids we have extended the study to include several bases (B) of different alkyl chain length from no side chain in ammonia (NH₃) (all PILs) to methylamine (MA) and butylamine (BA) (Table 1).

The PILs were prepared by reaction of an equimolar (slight amine excess) amount of acid and base, either neat or in an aqueous solution, by dropwise addition of the acid to the amine at low temperature. Pure PILs were achieved after evaporation of any excess amine along with the water at 80 °C in vacuum using a rotary evaporator. For full details on preparation procedures as well as T_m , viscosity, density, and ionic conductivity measurements see ref 29. Note that the conductivity was measured by impedance spectroscopy and is thus always total ionic conductivity.

II.b. Ab initio Calculations. Ab initio calculations were used to optimize the geometries of the acid base pairs and their different components, starting from several initial structures, at the HF/6-31++G** level. Both protonated and deprotonated structures were optimized for all the acids and bases. The optimizations were followed by frequency calculations to make sure that the resulting structures were true minima. These structures were further optimized using the hybrid density functional B3LYP³⁰⁻³² and the electron correlation method MP2³³ with the same basis set. The results from the three calculational models are in excellent agreement and we here only present the results from the MP2 calculations, as electron correlation has been found to be important for materials with proton transfer and hydrogen bonds.^{34,35}

The energy difference (ΔE) for transferring the proton was calculated as the difference in total energy of proton transferred acid-base system and the acid-base system:

$$\Delta E = E(A^- + BH^+) - E(AH + B) \quad (1)$$

The interaction enthalpy ΔH_{int} of an ion pair was calculated as the difference in sum of the total energy and the electronic and thermal enthalpies at 298.15 K of the two ions and of the most stable ion pair (eq 2). For vacuum calculations, the difference between E and H is very small and consist mainly of the zero point energy and $k_B T$.³⁶ The interaction enthalpy is positive in our calculations because the energy of ions in the gas phase is much less favorable than for neutral molecules.

$$\Delta H_{int} = H(A^-) + H(BH^+) - H(A-H-B) \quad (2)$$

Solvation free energies for the ions were calculated at 298.15 K by a continuum method (CPCM)^{37,38} using a predefined solvent with a dielectric constant of 10.36 (CH₂ClCH₂Cl). The

continuum method is used to reduce the effect of performing the calculations in vacuum.

ΔG_{solv} is defined as the sum of the solvation free energies of the two ions. In the work of Krossing et al. their ILs dielectric constant (ϵ) varied between 10 and 15 and their ΔG_{solv} was calculated by continuum quantum mechanical methods using measured ϵ of each IL obtained from dielectric spectroscopy.¹⁶ In their work the dielectric constant was used as one parameter for prediction of the exact melting point. They also used the melting point value to predict ϵ . In our calculations however, we only use the solvation method, with a predefined solvent, as a tool to get a rough estimate of the solvation energy. Calculating ΔG_{solv} for the $\epsilon = 10$ and $\epsilon = 20$ for our PILs results in a systematic shift in ΔG_{solv} for our ions of $\sim 20 \text{ kJ mol}^{-1}$, which according to Krossing et al. in the worst case scenario can shift the melting temperature prediction 20–30 °C.

The volume of each specie was calculated by a Monte Carlo integration method inside a contour of $0.001 \text{ e bohr}^{-3}$ density. The volume was calculated 7 times to get a statistically reliable value (mean standard deviation of 6%). The total volume was obtained by adding the values of the two ions. The theoretical molecular density was calculated by taking the ratio of the molar mass of the ions (in u) divided by the calculated volume of the ion pair (in bohr^3). All quantum mechanical calculations were performed using the Gaussian 03 software.³⁶

II.c. Thermodynamic Calculations. The free energy of fusion (ΔG_{fus}) was calculated by a method developed by Krossing et al.:¹⁶

$$\Delta G_{\text{fus}}^T = \Delta G_{\text{latt}}^T + \Delta G_{\text{solv}}^{298.15} + \Delta G_{\text{corr}} \quad (3)$$

Here $\Delta G_{\text{latt}}^T = \Delta H_{\text{latt}}^T - T\Delta S_{\text{latt}}^T$, where the lattice enthalpies and entropies are obtained using volume based empirical formulas from refs 39 and 40. ΔS_{latt}^T is obtained as the difference between the lattice entropy (at 298.15 K) and the sum of the gas-phase entropies of the ions at the specific temperature (T). The solvation free energy (ΔG_{solv}) is calculated by continuum methods (for details see above) in the thermodynamic cycle described in ref 16. The magnitude of ΔG_{solv} is in the same level as ΔG_{latt} whereas ΔG_{corr} is only a minor correction parameter to compensate for calculating the ΔG_{solv} at room temperature, and not at the actual melting temperature (for details see ref 16).

We also used a variation of the method above where the ΔH_{latt} was exchanged by the interaction enthalpy ΔH_{int} (see eq 2) to obtain the free energy of fusion $\Delta G_{\text{fus(int)}}$. The temperature for which $\Delta G_{\text{fus}} = 0$ is the predicted T_m for each method.

III. Results and Discussion

First we compare our computed volumes with volumes obtained from density measurements. Second we present results of T_m of the PILs and compare our results with those obtained earlier for ILs¹⁶ and discuss the factors that influences T_m . Third we turn to conductivity and present a hypothesis on how to construct a PIL with high conductivity.

As many of the parameters used in this work are based on molecular volumes, it is especially important to know how reliable are the calculated volumes. We present results for both mono- and polysubstituted alkylamine based PILs. That is where substitution of one or several hydrogen atoms on the amine by an alkyl chain of up to four carbon atoms in the backbone. The ab initio computed volumes were compared with the actual volumes of 15 PILs obtained from density measurements. As can be seen in Figure 1 the gas-phase calculations give an

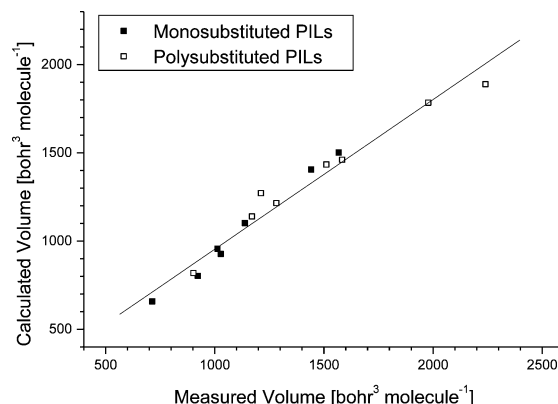


Figure 1. Correlation of computed volumes and volumes obtained from density measurements, the line is the best linear fit ($y = (0.85 \pm 0.04)x + 105 \pm 62$).

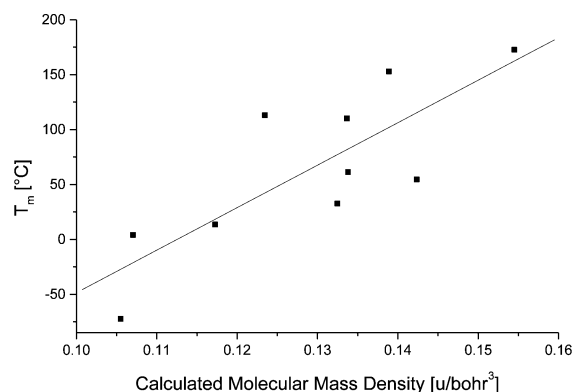


Figure 2. T_m versus the calculated molecular mass density for PILs based on EA (std deviation = 47 K).

excellent description of the volumes even in condensed phase media. (The standard deviation is $\sim 6\%$.) Thus we can use the calculated volumes for our correlations from now on. Adding together the volumes of the individual ions gave a larger total volume and thus a better description of the condensed media volume than using the calculated volume of an ion pair. Our calculated volumes are smaller than the corresponding measured PIL volume but larger than the volumes obtained from crystal data.^{41–43} The fact that we have very good agreement between calculated and measured volumes implies that the electron density cut off used in the calculations reflects the packing density of the PIL in the condensed phase, or that the compression from the electrostatic forces eliminates the packing spare space.

In Table 1 we present experimental data of T_m for all PILs and it can be observed that the influence of the acid is most significant. Our starting point for the investigation of the origin of this difference is to relate to the density of the PILs by using the molecular weights and the calculated sizes of the PILs. The crystallization and melting of a PIL should depend on the packing properties of the ions and their pairwise interactions.⁴⁴ For the ethylammonium based PILs, the main focus of this paper, the general trend is increasing T_m with increasing molecular mass density, Figure 2. It must be noted that there is some scatter in the data. In the calculation of the molecular density we have used the volume of one ion pair. However, this volume does not differ significantly from the sum of the volume of the isolated ions, which means that important shape parameters influencing the packing are lost. As a consequence this density parameter cannot be used to explain the influence of side chain length variations of the cation. Our calculated

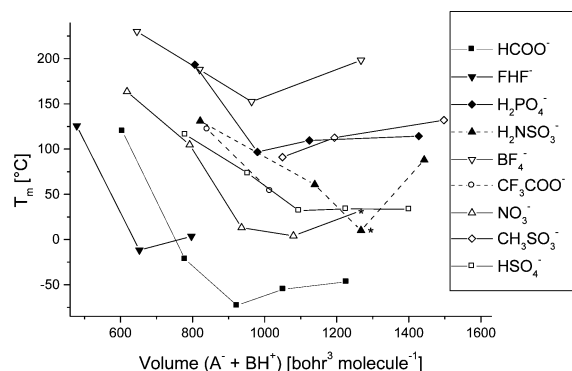


Figure 3. T_m versus volume ($A^+ + BH^+$) for the PILs. Each line connects a sequence of PILs with identical anions and varying cation side chain length. The two sequences with dotted lines lack T_m values of the MA PILs. T_m values for propylamine PIL are added for nitrate,⁴⁹ formate, hydrogen sulfate, and sulfamate. For the propylamine PILs of the nitrate and the sulfamate as well as the butylammonium nitrate, the T_m values (marked with *) are experimentally uncertain.

density values decrease gradually with increasing alkyl side chain of the base, which is not the case for the corresponding T_m .

For the cation side chain influence, the volume in itself seems to be a more important parameter. This can be seen in Figure 3 where the T_m dependence of the cation for each anion is investigated. We observe a decrease in T_m for all systems from the symmetric ammonia to methylamine. For all PILs except those with FHF^- , $H_2PO_4^-$, and $CH_3SO_3^-$ anions T_m decreases as the alkyl chain length increases, through a minimum for the ethylammonium PILs, before a final increase. Three PILs lack methylammonium base T_m data, Table 1.

Using the volume correlation also for different anions, the T_m dependence on volume grows with the size of the cation from being almost independent in the case of ammonia to a very strong dependence for the butylamine PILs, Figure 4a–d. The higher symmetry of the ammonium cation is believed to cause the significantly higher melting temperatures of its corresponding PILs. (The same high symmetry can be the reason why all BF_4^- -based PILs have higher T_m than expected from the volume data.)

Simple volume based correlations give some insight into the T_m dependencies of PILs. It is, however, likely that even more could be gained by turning to the laws of thermodynamics:

$$\Delta G = \Delta H - T\Delta S \quad (4)$$

The free energy (G) has to be lower in the liquid state than in the crystal for the PIL to melt. The enthalpy contribution for salts (ΔH), mainly the lattice energy, has for aprotic ILs recently been shown to be approximately proportional to the inverse of the cube root of volume.⁴⁵ For the entropies, Glasser reported on a linear increase in ΔS with volume of the ions in aprotic ILs.⁴⁶ The variation in the literature data, from which the relation is based, is however substantial, reporting both increasing and decreasing ΔS with increasing ion size for short cation side chains, whereas predominantly increasing ΔS for longer side chains.⁴⁶ Applying these volume based lattice enthalpies and entropies to our PILs implies that bigger ions should give a lower T_m . Figure 4, however, shows the opposite trend for all the monosubstituted alkylamine bases, which implies that ΔS must have a size dependence larger than the enthalpy, a dependency that becomes stronger with increased alkyl chain length or that another important parameter is missing.

As discussed above an increase in cation size does not influence T_m the same way as the anion size does. It is thus

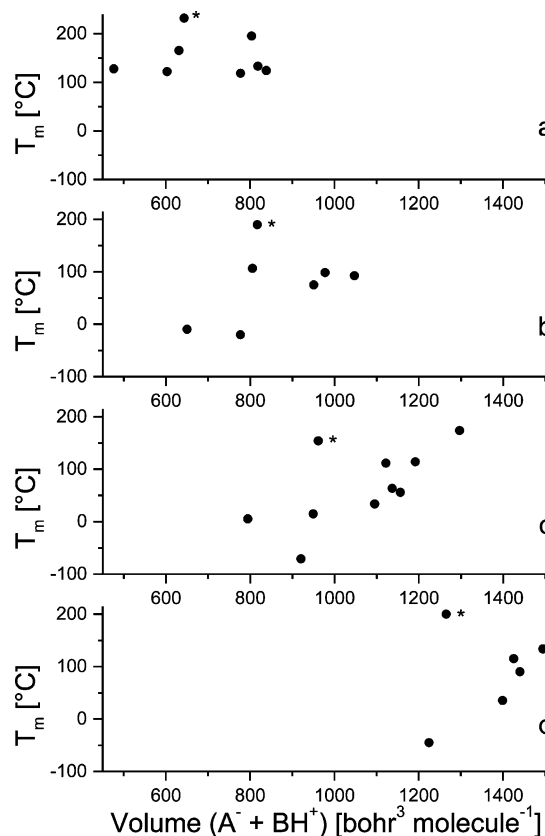


Figure 4. T_m versus volume ($A^+ + BH^+$) for (a) ammonia based PILs, (b) MA based PILs, (c) EA based PILs, and (d) BA based PILs, respectively. The PIL with BF_4^- as the anion (marked with *) has a T_m higher than the trend-line for all cations.

likely that the cation size influences ΔS more than it does ΔH , for protic systems and has a maximum value for a certain side chain length. This is reasonable in systems where the volume of the anion and cation is on the same size order, as increasing the length of the cation side chain results in an increase in the degrees of freedom (dof), $dof \sim 3N$, where N is the number of atoms. The increase will continue until the available free volume of the system is more or less used and the side chain flexibility is restricted by contacts with their neighbors. When the side chains are longer, they will also start to interact more strongly with each other by van der Waals interactions, which increase the melting temperature.⁴⁷ Our data show this behavior for all individual acids when the length of the base alkyl chain is increased, Figure 3. All PILs show approximately the same curvature with a minimum T_m for an alkyl chain length of 1–3 methylene units. A maximum value of ΔS , and consequently a minimum in T_m , for the ethyl side chain length in 1-alkyl-3-methyl-imidazole bis(trifluoromethanesulfonyl)imide aprotic ILs have recently been reported by Tokuda et al.⁴⁸ in agreement with our T_m data.

The same reasoning can, however, not explain the variation in T_m seen in Figure 4 for the different acids, as the dof of the acids should be comparable. It is thus more likely that the reason for the difference in T_m with anion variation should be a consequence of ΔH . It is argued that in a liquid system, with uniformly distributed ions of opposite charge, a Madelung energy develops that is comparable to that of the corresponding crystal.¹⁰ This energy can, however, differ in our systems as the degree of proton transfer in the different PILs can vary in contrast to aprotic ILs where all systems are fully ionic. Therefore the simple lattice energy formula used for aprotic ILs might be inapplicable to PILs.

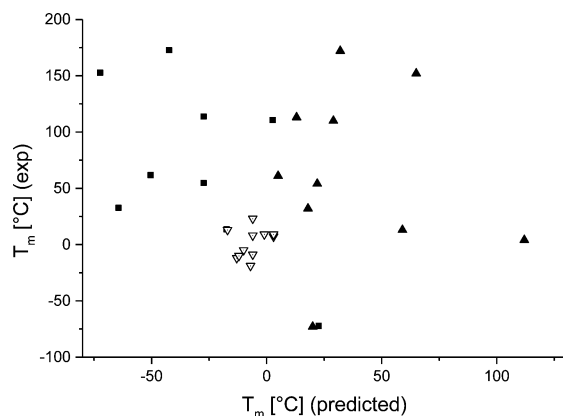


Figure 5. T_m (experimental) versus T_m predicted for EA based PILs using Krossing's method¹⁶ (filled triangles) and our method with ΔH_{int} (squares). Also shown are the aprotic IL data taken from ref 16 (open triangles).

As previously mentioned, Krossing et al. very recently used a third parameter, the free energy of solvation (ΔG_{solv}) together with the lattice enthalpy and the entropy from Glasser's approach to explain the melting temperature in aprotic ILs.¹⁶ In their work they used ΔG_{solv} calculated by continuum methods with the use of measured ϵ of each IL obtained from dielectric spectroscopy.¹⁶ Assuming roughly similar ϵ for the PILs as for the ILs and using a solvent with ϵ similar to the ILs discussed above for all PILs we can get a rough estimate on how ΔG_{solv} varies in our systems. This is possible as the variations in ΔG_{solv} between the different ions are larger than the difference of ΔG_{solv} calculated by different ϵ . The ΔG_{solv} for the series of alkylammonium ions is most negative for the ammonium ion and increases gradually until it converges to a constant value for BuNH_3^+ and cations with longer side chains. The variations in ΔG_{solv} for the anions are slightly higher than for the cations ($\sim 70 \text{ kJ mol}^{-1}$ to be compared with 45 kJ mol^{-1} for the cations). Applying Krossing's method to our PILs does not give any correlation with the experimentally obtained T_m (Figure 5). The scatter in our T_m data is still comparable to the data reported by Krossing. It is not surprising that the deviation of the predicted from the experimental T_m is large using Krossing's approach, because the general trend is increasing T_m with the increasing size of the anions. Regarding the cation dependence, because ΔG_{solv} is most negative for the ammonium PILs and increases for cations with a longer alkyl chains, this approach predicts an increasing T_m decrease with increasing alkyl chain length for all the PILs, instead of a minimum T_m for a relatively short alkyl chain as seen by experiments.

In an attempt to improve the model, we calculated the interaction enthalpy ΔH_{int} (eq 2) by ab initio methods. This approach, however, does not improve anything (Figure 5), rather it also predicts the wrong trend when ΔH_{int} and T_m are compared. The ability to form ions, i.e., to transfer the proton, is also likely to be important for the melting temperature as it affects the number of charged species and hence the interactions. Using ΔH_{int} for the interaction energy does not take the degree of proton transfer into account and is thus a likely source of error. We correlate the ability to form ions to ΔE (eq 1), where an ionic system with a small ΔE value is more stable than one with a large ΔE value. Using ΔE together with our interaction enthalpy ($\Delta H_{\text{int}} - \Delta E$) as a measure of the interaction energy produces a correct general T_m trend. This new interaction energy, however, is much lower and can therefore not be used in the thermodynamic cycle to predict the true T_m . The third parameter in Krossing's approach, ΔG_{solv} , is indeed an important parameter

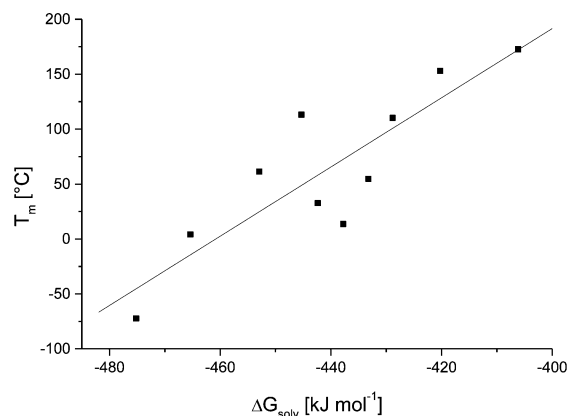


Figure 6. T_m versus ΔG_{solv} for EA based PILs (std deviation = 39 K).

also for PILs. In fact, a plot of T_m vs ΔG_{solv} gives roughly linear dependence for ethylamine based PILs, Figure 6. The standard deviation for this correlation is of the same order as for the density correlation, Figure 2. This correlation is also applicable to the PILs based on ammonium, methylammonium and butylammonium when the anion is varied.

A PIL that has a much more positive ΔE value than the others is ethylammonium formate (EAFm). EAFm also has a very low T_m , which likely is caused by the low degree of proton transfer, i.e., a low ionic character in the solid material. This difference between EAFm and the rest of the PILs can be exemplified by comparing the difference between the arithmetic mean of the T_m for the pure acid and base and that of the T_m of the PIL, ΔT_m , and their corresponding ΔE , Table 1. All PILs but EAFm (and to some extent ethylammonium sulfamate that is solid up to 200°C where it decomposes) have positive values of ΔT_m , which is expected when a salt is formed. Furthermore, EAFm does not show a one-step weight loss (TGA) as the other PILs,²⁹ but instead a two-step process. This is the typical behavior of a binary liquid mixture with non-negligible vapor pressure. ΔE is thus important for the classification into poor or good ionic liquids with respect to ionicity.

The working temperature, limited by the liquid range, is not the sole important property of a PIL for FC applications—conductivity is just as important. The T_m values for the studied PILs span over 200°C with nonmatching temperature windows of the liquid state, and their conductivities can therefore not be compared at a common temperature. Furthermore, the conductivity is very dependent on the viscosity, as can be seen in Figure 7 (inset). To be able to compare the PILs and to compensate for the viscosity dependence, we use the conductivity at a common viscosity η , namely 1.2 mPa s , (“ η -scaled conductivity”). This way we decouple the viscosity dependence and only look at the ionic conductivity. A drawback of this approach is that the conductivity is for different temperatures, which might affect the equilibrium constant of proton transfer: at high temperature the PIL is closer to the temperature where the proton is transferred back to the acid. This might influence the possibility of the Grotthuss mechanism for the different systems as an intermediate number of protons might be transferred at that specific temperature resulting in a higher probability of reversible transfer between the sites.

Viscosity data exist for three PILs (ethylammonium nitrate (EAN), ethylammonium hydrogen sulfate (EAS), and EAFm); for these the maximum η -scaled conductivity is found for EAN, closely followed by EAS, and a clear jump down to EAFm, Figure 7. The most probable explanation of the lower conductivity of EAFm is the lower degree of proton transfer and, as a

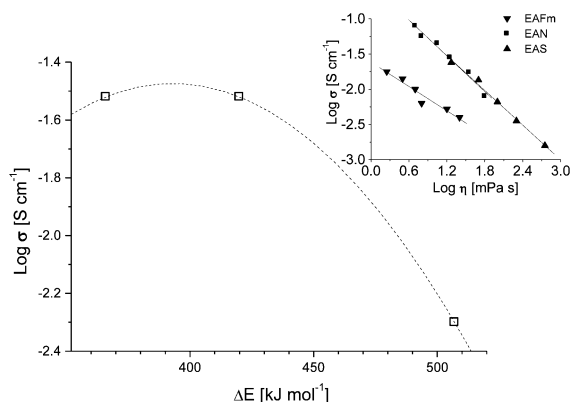


Figure 7. $\log(\sigma)$ at constant viscosity versus ΔE for, from left to right, EAS, EAN, and EAFm, respectively. The line is an x^2 fit given to guide the eye. Inset: $\log(\sigma)$ vs $\log(\eta)$ for the same three PILs. Lines are linear fit to data.

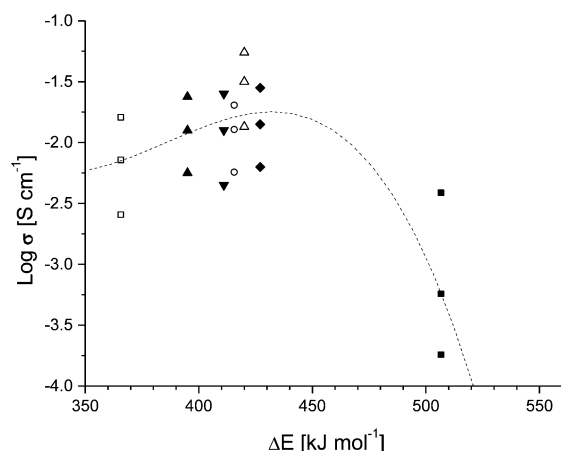


Figure 8. $\log(\sigma)$ at $T_m + 10$ °C, $+ 30$ °C, and $+ 60$ °C vs ΔE for EA based PILs. See Figure 3 for explanation of symbols. The line is an x^3 fit given to guide the eye.

consequence, fewer charge carriers contributing to the conductivity. Consequently, EAS should have a higher charge carrier concentration than EAN. However, this is dependent on the relation between the value of ΔE and ideal ΔE for a complete proton transfer. The observed lower conductivity might be due to the slower diffusion of HSO_4^- (EAS) than NO_3^- (EAN), based on anion size. It can also be an indication that another transport process is present in PILs, apart from the vehicular, and that this transport process changes with ΔE . An intermediate ΔE value (as for EAN) should, however, give a degree of proton transfer that possibly maximizes conductivity as the number of charge carriers are high and simultaneously some sites are available for the Grotthuss type transport. If the temperature at which the conductivity is measured influences the type of transport in the PIL, it would in fact favor EAS rather than EAN, as a higher temperature above the corresponding T_m is needed for EAS to get the same viscosity as EAN. If data points should be available for systems with even lower ΔE , the conductivity is expected to converge to a constant value for all fully ionic systems. Thus ΔE seem to be a prominent factor determining the higher conductivity PIL at constant viscosity.

Another approach to compare the conductivities, also attainable for PILs with no available viscosity data, is to use the conductivity at the same temperature above T_m ($+10$, $+30$, and $+60$ °C). The same behavior, as for constant viscosity, is found with a maximum conductivity for EAN, Figure 8. Here we have fitted the data with an x^3 -curve. Motivated by that, a decrease in conductivity for smaller ΔE indicated is not very likely, as

an even smaller ΔE arguably should not give a significantly more ionic system. To obtain a PIL with high conductivity, the magnitude of ΔE must be reasonably high; otherwise, the system will have low ionicity. The observed trend in conductivity could simply be a measure of the viscosity, but EAFm having a very low viscosity clearly contradicts this. On the other hand, ΔE could also be an important factor for the viscosity for all PILs that are not fully ionic, as it is a measure of the ionic interactions, whereas for fully ionic systems the viscosity should be independent of ΔE .

IV. Conclusions

The T_m of PILs cannot be estimated by the same approach as recently proposed for aprotic ILs by Krossing et al., probably due to a bad description of the PIL lattice energy by this method. Still the T_m of a specific PIL is to a large extent determined by the size of its anions and cations. For any given anion the PIL melting temperature has a minimum for a monosubstituted alkylamine of a chain length of 1–3 carbon atoms. The PILs generally have higher melting temperatures the larger their anion size. Another important parameter is the solvation energy that preferably for low melting PILs should have a large negative value for the ingoing ions. Thus, by considering the density, volume, and ΔG_{solv} of the ions, it is possible to choose the beginning of the working temperature range (T_m) for PIL based electrolytes by changing the size of the ingoing ions. Depending on ΔE the PIL will keep its ionic character all the way up to the decomposition temperature. ΔE is important not only for the decomposition temperature but also for the ionicity of the PIL and hence their conductivity.

Acknowledgment. Financial support from the Royal Swedish Academy of Science, Stiftelsen Futura, Karl and Annie Leons memorial fund, and Wilhelm and Martina Lundgrens Science Foundation are greatly acknowledged.

Supporting Information Available: Additional data from the calculations are given as Supporting Information, including thermodynamic data, solvation energies, volumes of ions, and graphs of T_m vs ΔG_{solv} , and T_m vs $\Delta H - \Delta E$. This material is available free of charge via the Internet at <http://pubs.acs.org>.

References and Notes

- (1) Wasserscheid, P.; Keim, W. *Angew. Chem., Int. Ed.* **2000**, *39*, 3772.
- (2) Earle, M. J.; Seddon, K. R. *Pure Appl. Chem.* **2000**, *72*, 1391.
- (3) Ohno, H. *Electrochemical Aspects of Ionic Liquids*; John Wiley & Sons, Inc.: New York, 2005.
- (4) Shin, J.-H.; Henderson, W. A.; Passerini, S. *J. Electrochem. Soc.* **2005**, *152*, A978.
- (5) Bansal, D.; Cassel, F.; Croce, F.; Hendrickson, M.; Plichta, E.; Salomon, M. *J. Phys. Chem. B* **2005**, *109*, 4492.
- (6) Xu, W.; Angell, C. A. *Science* **2003**, *302*, 422.
- (7) Susan, M. A. B. H.; Noda, A.; Mitsushima, S.; Watanabe, M. *Chem. Commun.* **2003**, *8*, 938.
- (8) Belières, J.-P.; Gervasio, D.; Angell, C. A. *Chem. Commun.* **2006**, *46*, 4799.
- (9) Belières, J.-P. *Protic Ionic Liquids, High Temperature Electrolytes for Fuel Cell Applications*. Ph.D. Thesis, Arizona State University, 2005.
- (10) Yoshizawa, M.; Xu, W.; Angell, C. A. *J. Am. Chem. Soc.* **2003**, *125*, 15411.
- (11) van Grotthuss, C. J. D. *Ann. Chim.* **1806**, *58*, 54.
- (12) Turner, E. A.; Pye, C. C.; Singer, R. D. *J. Phys. Chem. A* **2003**, *107*, 2277.
- (13) Lee, S. U.; Jung, J.; Han, Y. K. *Chem. Phys. Lett.* **2005**, *406*, 332.
- (14) Tsuzuki, S.; Tokuda, H.; Hayamizu, K.; Watanabe, M. *J. Phys. Chem. B* **2005**, *109*, 16474.
- (15) Glasser, L.; Jenkins, H. D. B. *Chem. Soc. Rev.* **2005**, *34*, 866.
- (16) Krossing, I.; Slattery, J. M.; Daguene, C.; Dyson, P. J.; Oleinikova, A.; Weingartner, H. *J. Am. Chem. Soc.* **2006**, *128*, 13427.

- (17) Ngo, H. L.; LeCompte, K.; Hargens, L.; McEwen, A. B. *Thermochem. Acta* **2000**, 357–358, 97.
- (18) Hirao, M.; Sugimoto, H.; Ohno, H. *J. Electrochem. Soc.* **2000**, 147, 4168.
- (19) Bicak, N. *J. Mol. Liq.* **2005**, 16, 15.
- (20) Ohno, H.; Yoshizawa, M. *Solid State Ionics* **2002**, 154–155, 3003.
- (21) Yang, C.; Costamagna, P.; Srinivasan, S.; Benziger, J.; Bocarsly, A. B. *J. Power Sources* **2001**, 103, 1.
- (22) Deng, W. Q.; Molinero, V.; Goddard, W. A., III. *J. Am. Chem. Soc.* **2004**, 126, 15644.
- (23) Aylward, G.; Findlay, T. *SI Chemical data*; John Wiley & Sons: Milton, Australia, 2002.
- (24) Dean, J. A. *Lange's Handbook of Chemistry*, 15th ed.; McGraw-Hill: New York, 1999; pp Chapter 8.
- (25) Lide, D. R., Ed. *CRC Handbook of Chemistry and Physics*, 76th ed.; Boca Raton, FL, 1995–1996.
- (26) Zemva, B. *Compt. Rend. Acad. Sci., Ser. IIc: Chim.* **1998**, 1, 151.
- (27) Gillespie, R. J.; Liang, J. *J. Am. Chem. Soc.* **1988**, 110, 6053.
- (28) Olah, G. A.; Surya Prakash, G. K.; Sommer, J., Eds. *Superacids*; John Wiley & Sons: New York, 1985; Chapter 1.
- (29) Belières, J.-P.; Angell, C. A. *J. Phys. Chem. B* **2007**, 111, 4926.
- (30) Lee, C.; Yang, W.; Parr, R. G. *Phys. Rev. B* **1988**, 37, 785.
- (31) Becke, A. D. *J. Chem. Phys.* **1993**, 98, 5648.
- (32) Vosko, S. H.; Wilk, L.; Nusair, M. *Can. J. Phys.* **1980**, 58, 1200.
- (33) Möller, C. M.; Plesset, M. S. *Phys. Rev.* **1934**, 46, 618.
- (34) Alavi, S.; Thompson, D. L. *J. Phys. Chem. A* **2004**, 108, 8801.
- (35) Del Bene, J. E.; Jordan, M. J. T. *J. Mol. Struct. (THEOCHEM)* **2001**, 573, 11.
- (36) Frisch, M. J.; Trucks, G. W.; Schlegel, H. B.; Scuseria, G. E.; Robb, M. A.; Cheeseman, J. R.; Montgomery, J. A., Jr.; Vreven, T.; Kudin, K. N.; Burant, J. C.; Millam, J. M.; Iyengar, S. S.; Tomasi, J.; Barone, V.; Mennucci, B.; Cossi, M.; Scalmani, G.; Rega, N.; Petersson, G. A.; Nakatsuji, H.; Hada, M.; Ehara, M.; Toyota, K.; Fukuda, R.; Hasegawa, J.; Ishida, M.; Nakajima, T.; Honda, Y.; Kitao, O.; Nakai, H.; Klene, M.; Li, X.; Knox, J. E.; Hratchian, H. P.; Cross, J. B.; Bakken, V.; Adamo, C.; Jaramillo, J.; Gomperts, R.; Stratmann, R. E.; Yazyev, O.; Austin, A. J.; Cammi, R.; Pomelli, C.; Ochterski, J. W.; Ayala, P. Y.; Morokuma, K.; Voth, G. A.; Salvador, P.; Dannenberg, J. J.; Zakrzewski, V. G.; Dapprich, S.; Daniels, A. D.; Strain, M. C.; Farkas, O.; Malick, D. K.; Rabuck, A. D.; Raghavachari, K.; Foresman, J. B.; Ortiz, J. V.; Cui, Q.; Baboul, A. G.; Clifford, S.; Cioslowski, J.; Stefanov, B. B.; Liu, G.; Liashenko, A.; Piskorz, P.; Komaromi, I.; Martin, R. L.; Fox, D. J.; Keith, T.; Al-Laham, M. A.; Peng, C. Y.; Nanayakkara, A.; Challacombe, M.; Gill, P. M. W.; Johnson, B.; Chen, W.; Wong, M. W.; Gonzalez, C.; and Pople, J. A. *Gaussian 03*, revision C.02; Gaussian, Inc.: Wallingford, CT, 2004.
- (37) Barone, V.; Cossi, M. *J. Phys. Chem. A* **1998**, 102, 1995.
- (38) Cossi, M.; Rega, N.; Scalmani, G.; Barone, V. *J. Comput. Chem.* **2003**, 24, 669.
- (39) Jenkins, H. D. B.; Roobottom, H. K.; Passmore, J.; Glasser, L. *Inorg. Chem.* **1999**, 38, 3609.
- (40) Jenkins, H. D. B.; Glasser, L. *Inorg. Chem.* **2003**, 42, 8702.
- (41) Choi, C. S.; Mapes, J. E.; Prince, E. *Acta Crystallogr.* **1972**, B28, 1357.
- (42) Caron, A. P.; Ragle, J. L. *Acta Crystallogr.* **1971**, B27, 1102.
- (43) Henderson, W. A.; Fylstra, P.; Johansson, P.; De Long, H. C.; Trulove, P. C.; Parsons S. Manuscript in preparation.
- (44) Trohalaki, S.; Pachter, R. *QSAR Comb. Sci.* **2005**, 24, 485.
- (45) Gutowski, K. E.; Holbrey, J. D.; Rogers, R. D.; Dixon, D. A. *J. Phys. Chem. B* **2005**, 109, 23196.
- (46) Glasser, L. *Thermochim. Acta* **2004**, 421, 87.
- (47) Holbrey, J. D.; Seddon, K. R. *J. Chem. Soc., Dalton Trans.* **1999**, 2133.
- (48) Tokuda, H.; Hayamizu, K.; Ishii, K.; Susan, M. A. B. H.; Watanabe, M. *J. Phys. Chem. B* **2005**, 109, 6103.
- (49) Poole, C. F.; Kersten, B. R.; Ho, S. S. J.; Coddens, M. E.; Furton, K. G. *J. Chromatogr.* **1986**, 352, 407.